J Musculoskel Neuron Interact 2003; 3(1):8-16

Original Article

Hylonome

Myostatin expression in age and denervation-induced skeletal muscle atrophy

A.P. Baumann, C. Ibebunjo, W.A. Grasser, V.M. Paralkar

Cardiovascular and Metabolic Diseases, Groton Laboratories,
Pfizer Global Research and Development, Groton, CT, USA

Abstract

Myostatin is hypothesized to regulate skeletal muscle mass and to be a potential target for therapeutic intervention in sarcopenia. To clarify whether myostatin is invariably associated with sarcopenia, this study examined the levels of expression of myostatin mRNA and protein in Sprague Dawley rats during aging- and denervation-induced sarcopenia. The level of myostatin mRNA in the gastrocnemius decreased progressively with age being 9, 34 and 56% lower at 6, 12 and 27 months, respectively, compared with mRNA levels at 1.5 months. In contrast, two low molecular mass isoforms of myostatin protein identified by Western blotting increased progressively with age. With denervation, myostatin mRNA was 31% higher on day 1 but by 14 days after sciatic neurectomy when the muscle had atrophied 50%, myostatin expression decreased 34% relative to the sham operated limb. Western analysis of the denervated gastrocnemius showed that myostatin protein levels varied in parallel with mRNA. These disparate patterns of expression of myostatin during age- and denervation-induced atrophy suggest that the regulation of myostatin is complex and variable depending on whether the atrophy is slowly or rapidly progressive.

Keywords: Sarcopenia, Aging, TGF-β Superfamily, Growth and Differentiation Factor 8 (GDF-8)

Introduction

The transforming growth factor-β (TGF- β) superfamily members are structurally related proteins that play important roles during embryonic development and in adult life. This family includes the inhibins, activins, Müllerian inhibiting substance, bone morphogenetic proteins (BMPs), as well as the growth and differentiation factors (GDFs)[1]. GDF-8, also known as myostatin, does not fall into any of the known sub-families such as the BMPs or the TGF-β subfamily. Northern blot analysis and *in situ* hybridization in developing embryos showed that GDF-8 expression was localized to developing somites in early stages, while in later stages of embryogenesis and in adulthood, it is localized predominantly in skeletal muscles. Myostatin expression has also been detected in mammary tissue, adipose tissue, and cardiac muscle using RT-PCR[2,3]. In keeping with the characteristics of this superfamily, myostatin has a signal peptide, a prodomain, and after cleavage the carboxy-terminal domain forms a homodimer. This dimeric species activates receptor serine-threonine kinases to initiate a signaling cascade that involves the Smad family of proteins[1].

Myostatin was originally described by McPherron and Lee based on the phenotype of the myostatin gene knockout mice. The skeletal muscles of myostatin null mice have a two to three-fold increase in mass over wild type littermates, with the increase in mass attributed to both an initial hyperplasia and a later hypertrophy of the constituent muscle fibers[4]. A similar, naturally occurring phenotype has been observed in cattle where a 20-25% increase in muscle mass is seen in the Piedmontese and Belgian Blue breeds. This hypermuscled phenotype has been linked to a point mutation or a deletion in exon 3 of the myostatin gene that results in inactive myostatin protein[5-7]. These data have led to the proposal that myostatin might be a negative regulator of skeletal muscle mass[4,8]. Further supporting this hypothesis are the findings that transgenic mice carrying a dominant negative form of myostatin display an increased skeletal muscle phenotype[9]; and that serum myostatin levels are elevated in AIDS patients with cachexia[10] and in patients with skeletal muscle atrophy following prolonged bed rest[11] or hip replace-

Corresponding author: Vishwas M. Paralkar, Cardiovascular and Metabolic Diseases, Groton Laboratories, Pfizer Global Research and Development, Eastern Point Road, MS8118W-234, Groton, CT 06340, USA
E-mail: vishwas_m_paralkar@groton.pfizer.com

Accepted 28 August 2002

ments[12]. More recently, Zimmers et al. have demonstrated in athymic nude mice that systemic overexpression of latent myostatin induced cachexia independent of tumor necrosis factor (TNF) and interleukin-6[13].

In contrast with the foregoing, experimental *in vivo* studies have yielded conflicting evidence. For example, 42% atrophy of the soleus muscle produced by 7 days of hind leg unloading in female mice was not associated with any detectable changes in myostatin mRNA expression. However, in the gastrocnemius-plantaris muscle complex of these same mice, the 17% decline in muscle mass at day 7 of hind leg unloading was preceded by a 67% elevation of myostatin mRNA levels at day 1 but no increase was observed at day 7. This suggested that myostatin expression was not strongly associated with muscle atrophy[14]. In contrast, 17 days of space flight that produced 19-24% atrophy of muscles of the lower hind leg in rats was associated with a 1.9 to 5-fold increase in myostatin mRNA and protein, consistent with myostatin being a negative regulator of muscle mass[15]. Also in the rat, a 16% atrophy of the plantaris muscle produced by 10 days of hind leg unloading occurred with a 110% and 37% increase in myostatin mRNA and protein, respectively[16]. When a daily 30-minute period of muscle loading was superimposed during the unloading period, the loss of muscle mass was totally prevented although the increase in myostatin expression was only blunted by 50%. It was concluded that although increases in myostatin accompany muscle atrophy, significant increases in myostatin do not necessarily produce muscle atrophy[16]. In another study, a slight elevation of myostatin protein was associated with 31-76% compensatory hypertrophy of the plantaris muscle produced by ablation of the synergistic soleus and gastrocnemius muscles, whereas a marked elevation was associated with denervation-induced atrophy of the soleus and plantaris muscles in the rat[17]. Similarly, myostatin mRNA level was elevated in the rat femoral muscle at 48 hours after bupivacaine injection[18]. However, others reported that both myostatin mRNA and protein levels decline in the soleus and extensor digitorum longus muscles of the rat by days 1-3 after bupivacaine injection followed by a return to levels at or above control muscles by day 7[19]. Further confounding the elucidation of the effects of myostatin on muscle mass in adult animals are the disparities in the size of the immunoreactive species of myostatin reported in both human and animal studies[10,15-17]. It is unclear to what extent these discrepancies are reflective of differences between species, muscles, or reagents, or whether they suggest diverse roles for myostatin in regulating muscle mass depending on the cause of the muscle atrophy. To date, despite much speculation on the potential utility of myostatin inhibitors to ameliorate the loss of muscle mass (sarcopenia) due to aging or disease (e.g., AIDS and cancer cachexia) there is a dearth of reports on the expression of myostatin in aged muscle. We have, therefore, investigated the changes in myostatin mRNA and protein expression in skeletal muscles during age-related as well as during denervation-induced muscle atrophy in the rat.

Materials and methods

Materials: All Taqman® reagents were from Applied Biosystems (Foster City, CA). Trizol®, Random Priming kit, SDS-PAGE gels, buffers and blotting membranes were from Invitrogen/Life Technologies (Carlsbad, CA). ^{32}P (α)- dATP, 3000 Ci/mmol, film and ECL® detection kit were from Amersham Pharmacia Biotech (Piscataway, NJ). Nytran® membrane was from Schleicher & Schuell (Keene, NH). All chemicals were from Sigma (St. Louis, MO). Protein detection reagent was from Bio-Rad (Hercules, CA). Secondary antibody was purchased from Jackson Immunoresearch (West Grove, PA).

Animals: Male Sprague Dawley (SD) rats aged 1.5, 6, 12, or 27 months (n=6 at each time point) were purchased from Harlan (Indianapolis, IN). They were allowed to acclimate to the vivarium for one week, sacrificed by CO_2 asphyxiation and the gastrocnemius, tibialis, plantaris, and soleus muscles of the lower hind leg were rapidly dissected out from both legs. Individual muscles were weighed, snap-frozen in isopentane cooled in liquid nitrogen and stored at -80ºC until processed.

In a separate study, 6-week-old male SD rats were purchased from Taconic Farms Inc. (Germantown, NY) acclimated to vivarium conditions for one week, weighed and randomized by body weight into 10 groups to undergo unilateral sciatic neurectomy (USN) or sham-USN. Surgical anesthesia was induced with isoflurane, the sciatic nerve was identified and lifted through an incision on the lateral aspect of the mid-thigh of one hind leg. For USN, a 1-cm segment of the sciatic nerve was excised whereas for sham-USN the nerve was not severed. The surgical incisions were closed and the animals were returned to their cages where recovery was uneventful. At day 0 (6-8 hr), 1, 4, 8, and 14 following the USN or sham-USN surgery, 6 rats per time point were sacrificed by CO_2 asphyxiation and the gastrocnemius, tibialis, plantaris, and soleus muscles from both the operated and contralateral non-operated limbs were rapidly dissected out. The individual muscles were weighed prior to freezing in isopentane cooled in liquid nitrogen and stored at -80°C until homogenization.

Quantitative PCR and Northern Blotting: A transverse block of sample, taken from the mid-belly of both heads of the gastrocnemius muscle (approximately 250 mg) was homogenized (n=6) in 3 ml Trizol® using a Brinkmann® polytron. Total RNA was processed per manufacturer's instructions plus a second stage purification as previously described[20]. Transcript abundance was analyzed by quantitative real-time PCR (Taqman®). RNA was reverse-transcribed per manufacturer's instructions using the Taqman® reverse transcription kit, which employs random hexamers. A control reaction in which the reverse transcriptase was omitted was also run. In addition to primers specific to the gene of interest, this methodology utilizes a quenched fluorescent-labeled probe that is positioned just downstream of the 5' primer. As DNA synthesis proceeds, the 5' exonucle-

ase activity of Taq polymerase degrades the probe, thus freeing the 5' fluorescent label from the quencher linked to the 3' end of the probe. Accumulation of fluorescence with cycle number is thus indicative of the relative transcript abundance. The following primers and probe were generated using Primer Express software (Applied Biosystems, Foster City, CA): 3' primer: CATTTGCAGTTTTTGCATCATT; 5' primer: ACATGCACTAATATTTCACTTGGCA; and dual-label probe: FAM-TCAAAAGCAAAAAGAA-GAAATAAGAACAAGGGAAA-TMRA. Primers were used at 900 nM, probe was used at 50 nM, and 50 ng of cDNA was used as a template for the amplification with Universal Master Mix for Taqman®. Reactions were run in triplicate in optical grade 96 well plates on a Perkin-Elmer 7700 instrument interfaced to Sequence Detector software. A control reaction lacking the sample template was also included. Reactions using an 18S primer/probe pair were run in parallel. Normalization and differences between samples were calculated using the $\Delta\Delta C_t$ (cycle threshold) method where $\Delta\Delta C_t$ equals (C_t sample 1 - C_t 18S sample 1) - (C_t sample 2 - C_t 18S sample 2)[21]. Percent change was calculated according to the following formulae: For upregulation, % increase = $(2\Delta\Delta C_t - 1) \times 100$; for downregulation, % decrease = $((1/\Delta\Delta C_t + 1) - 1) \times 100$.

For Northern blotting, 20 μg of total RNA was electrophoresed into a 1% agarose-formaldehyde gel, blotted onto a Nytran® membrane and hybridized as described previously[22,23] to a random primed ^{32}P (α) dATP 272 bp fragment (nt 1-272 of the coding region) of the murine myostatin gene (U84005). This region was chosen based on less sequence similarity to a related molecule, GDF-11. The low GC content of the probe necessitated using dATP for labeling. Washes were done as follows: 3 washes at room temperature in 1xSSC/0.1% SDS plus a final high stringency wash in 0.1xSSC/0.1% SDS at 55°C. The blot was exposed to both film and a phosphoimaging screen followed by quantitation using a Cyclone detector and Optiquant software. The blot was subsequently stripped by two 30-minute washes in boiling 0.1% SSC/0.1% SDS and rehybridized to an 18S rRNA probe using similar procedures. The level of expression of myostatin mRNA was normalized to that of the 18S rRNA in the same lane to account for differences in loading between lanes and experiments.

Western Blotting: A fraction of muscle (approximately 200-250 mg) was homogenized with a Brinkmann® polytron in 3 ml of 50 mM Tris-HCl, pH 7.4, 0.5 mM EDTA, 0.2% NP-40, 0.1% Triton X-100, 0.05% 2-mercaptoethanol, 1 mM sodium vanadate plus Boehringer Mannheim cOmplete™ protease inhibitor cocktail. Protein determinations were done by the Bradford method (Bio-Rad Laboratories, Hercules, CA) and 20 μg was loaded onto 14% Tris-Glycine gels and electroblotted. Blocking was carried out at 4°C for several hours in 5% nonfat dry milk in Tris-Buffered saline with 0.2% Tween 20 (TBS-T). The primary antibody (polyclonal) was raised in rabbits against the peptide NMLYFNGKEQIIYGKI and was used at 1 μg/ml after Protein A purification. This peptide sequence is located in the active carboxy-terminal domain (residues 350-365). Overnight incubation at 4°C in primary antibody was followed by three ten-minute washes in TBS-T. The secondary antibody, monoclonal peroxidase-conjugated donkey anti-rabbit IgG, $F(ab')_2$ was used at 1:10,000 for 2 hours at room temperature. After washing as described above in TBS-T, the blot was developed for one minute in ECL reagent and exposed to film (Amersham). The purified carboxy-terminal domain of murine myostatin expressed in *E. coli* was used as a control. To ensure selectivity of the polyclonal anti-myostatin antibody, a BLAST search was done with the peptide sequence above. The only molecule with significant similarity was a related Growth and Differentiation Factor, GDF-11, which when aligned with myostatin differs only by two amino acid residues. Therefore, the murine GDF-11 peptide, NMLYFNDKQQIIYGKI (differing amino acids underlined), was used to verify the specificity of the myostatin antibody used for Western blotting.

Statistical Analyses: Data are presented as mean ± SEM. One-way analysis of variance and the Scheffe test were used to compare differences in body and muscle weights and myostatin mRNA expression in the gastrocnemius muscle between the 1.5, 6, 12 and 27-month-old rats. For the USN study, the denervated limb was compared by paired t-test against the contralateral non-denervated limb that served as control, and values at the day 0 time-point were taken as baseline. $P < 0.05$ was considered to indicate statistically significant difference.

Results

Atrophy and Expression of Myostatin in Aged Gastrocnemius

In this study, we examined the expression of myostatin mRNA as a function of age. The ages of the rats studied (1.5, 6, 12 and 27 months) were chosen to represent growing, young adult, middle age and aged rats, respectively. Body weight and muscle mass peaked at about 6 months of age, and while body weight was maintained through 27 months of age, muscle mass declined to approximately 50% of the values in the 6 and 12-month-old animals (Figure 1). Because the myostatin mRNA levels were normalized to 18S, no further normalization to muscle mass was done. The amount of myostatin mRNA as quantified by real-time PCR using the Taqman assay and normalized to 18S rRNA expression declined progressively with age with levels at 6, 12 and 27 months being 9, 34 and 56% lower than levels at 1.5 months of age (Figure 2). Northern blot analysis of the gastrocnemius muscle also yielded similar results (Figure 3).

Western blot analysis of the gastrocnemius muscle revealed two isoforms of the active molecule (the carboxy-terminus that has undergone cleavage from the prodomain) of myostatin protein, one at 17 kDa and the other at 15 kDa. Two other species were also detected at 42 and 30 kDa (data not shown). Performing PAGE under more stringent reduc-

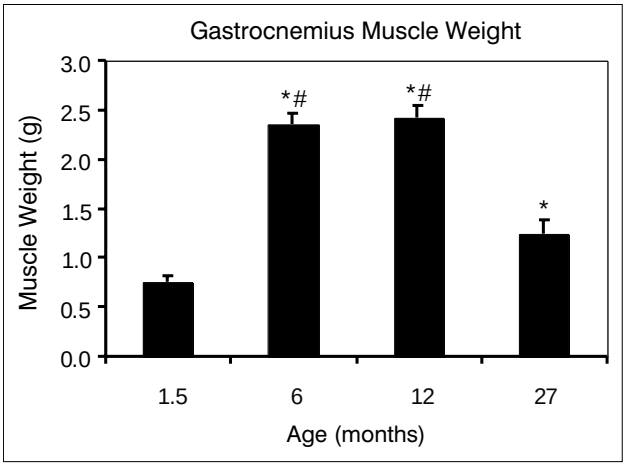

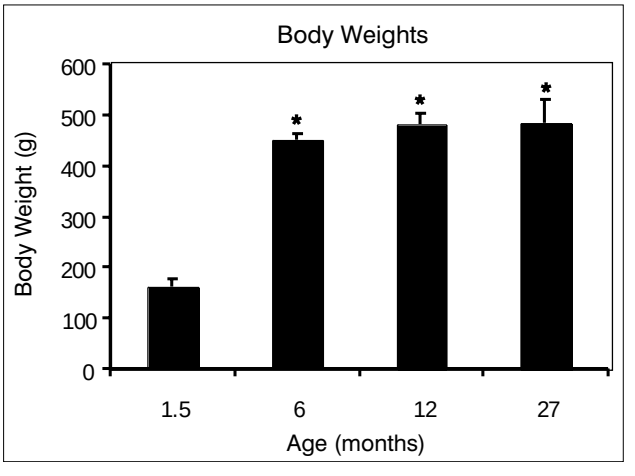

Figure 1. Changes in body weight and gastrocnemius muscle weight with age. Body weight and muscle weight peaked at about 6 months but whereas body weight was maintained, muscle weight had declined to ~50% of 12 month values by 27 months of age. * $P < 0.05$ versus 1.5 months; # $P < 0.0001$ versus 27 months (ANOVA and Scheffe's post hoc test, $n = 6$).

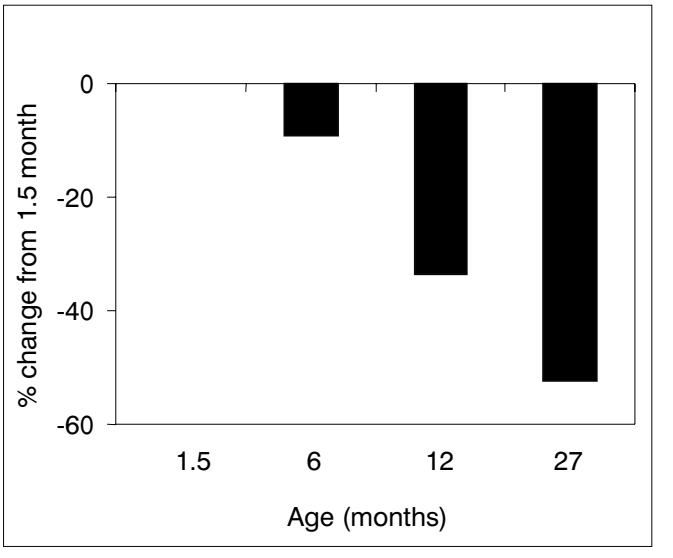

Figure 2. Myostatin mRNA levels decrease with age. mRNA from gastrocnemius was quantitated using real-time PCR following cDNA synthesis. A primer/probe set specific to the 5' end of the myostatin coding sequence was used to generate a 75bp amplicon. Data were generated according to the following formula: % decrease = $((1/\Delta\Delta C_t + 1)-1)x100$ where $\Delta\Delta C_t$ equals (C_t sample 1 - C_t 18S sample 1) - (C_t sample 2 - C_t 18S sample 2). As a result of this formula, the standard errors could not be calculated. Data are expressed as percent change from the 1.5-month-old baseline group (n=6).

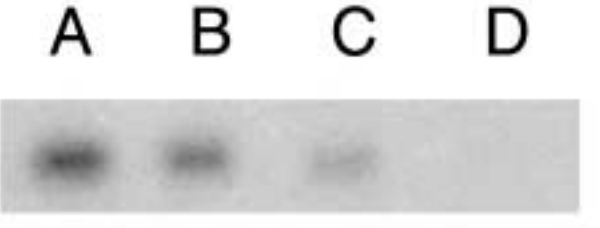

Figure 3. Northern blot analysis of gastrocnemius muscles from rats aged 1.5- (A), 6- (B), 12- (C) and 27-months (D). Twenty μg of total RNA was run on a 1% agarose-formaldehyde gel. The blotted RNA was hybridized to a 272 bp probe derived from the N-terminus of murine myostatin. Lanes shown are representative of n=3.

ing and denaturing conditions did not alter the migration of these species (data not shown) suggesting that the 30 and 42 kDa species represent incompletely reduced and unprocessed monomeric species of the protein, respectively. In contrast to the transcript, the expression of both the 15 and 17 kDa isoforms of myostatin protein was elevated at 27 months when compared with 1.5 months of age (Figure 4(A)). The carboxy-terminal domain of the murine myostatin that was expressed in *E. coli* and used as a positive control migrated predominantly at 17 kDa with a weak band at 30 kDa (data not shown). To rule out cross-reactivity with GDF-11, the GDF-11 peptide was subjected to SDS-PAGE and Western blot analysis alongside the GDF-8 peptide from which it differs by only two amino acids (see Materials and Methods). As shown in Figure 4(B), the antibody reacted with only the myostatin peptide. Taken together with the facts that the observed bands corresponded to the predicted molecular mass of the aforementioned species, and that the recombinant protein migrated similarly, this finding supports our conclusion that the visualized bands are indeed myostatin.

The level of expression of myostatin protein was also investigated in other muscles of the hind leg, namely the plantaris and tibialis anterior. In these muscles, only the

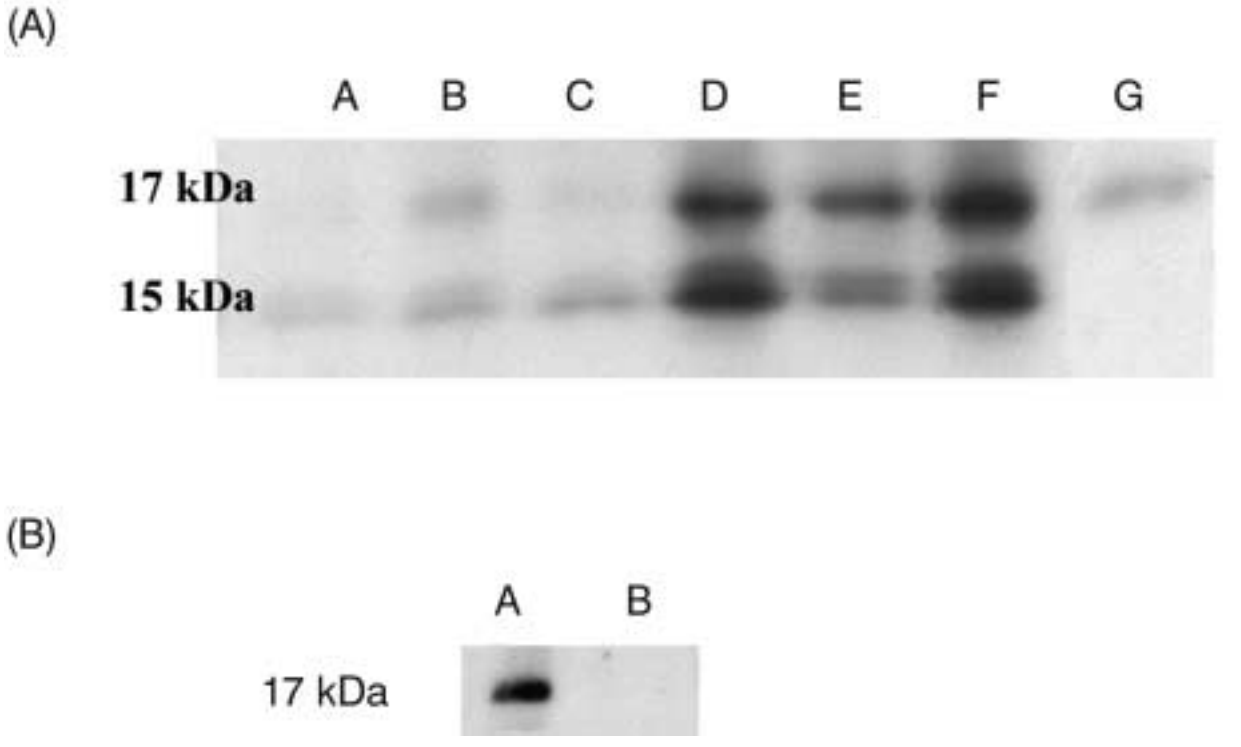

Figure 4. (A) Western blot showing levels of myostatin protein in gastrocnemius muscles from 1.5-month (lanes A-C) and 27-month-old rats (lanes D-F). Lane G is recombinant murine myostatin, C-terminal region, expressed in *E. coli*. (B) Western blot of myostatin peptide (NMLYFNGKEQIIYGKI; lane A) and GDF11 peptide (NMLYFNDKQQIIYGKI; lane B). Ten ng of each peptide was loaded onto a 14% Tris Glycine gel and analyzed as described under Materials and methods.

higher molecular mass species of the myostatin protein (30 and 42 kDa) were observed and the expression of these molecular species was increased with age (Figure 5).

Muscle Atrophy and Expression of Myostatin after Denervation

To further explore the regulation of myostatin during muscle atrophy, we examined myostatin expression during denervation-induced atrophy in young growing rats. Unilateral sciatic neurectomy (USN) in these rats did not affect their body weight gain but resulted in progressive atrophy of all leg muscles (irrespective of fiber type composition) in the USN leg relative to sham-USN or non-operated litter mate controls (Figure 6). Thus, by day 14 of USN all muscles, both fast and slow-twitch, had lost approximately 50% of their mass relative to their contralateral or sham-USN counterparts. USN and sham-USN did not alter the weight of muscles in the contralateral non-operated legs relative to age- and weight-matched controls (data not shown).

Myostatin mRNA levels in the gastrocnemius muscle as measured by Taqman PCR displayed a fluctuating pattern during the 14 day period (Figure 7). Initially, USN samples had 31% less message than their sham counterparts. It must be emphasized that the day-0 samples were taken approximately 6-8 hours after surgery or sham operation. Subsequently, the levels of myostatin message in operated animals compared with sham animals ranged from insignificant changes on days 1-8 to a 34% increase on day 14 post-surgery.

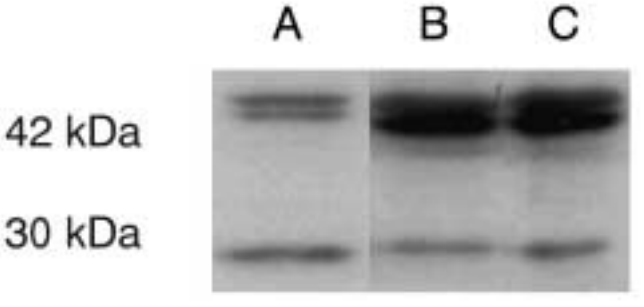

Figure 5. Myostatin protein expression in A) gastrocnemius, B) tibialis anterior, and C) plantaris muscles from 27-month-old SD rats (n = 2). In addition to the 30 kDa and 42 kDa species, a 15 kDa and 17 kDa species were also present in the gastrocnemius but not in the tibialis or plantaris muscles. Lanes shown are representative of the duplicate blots.

Western blotting of the gastrocnemius muscle revealed

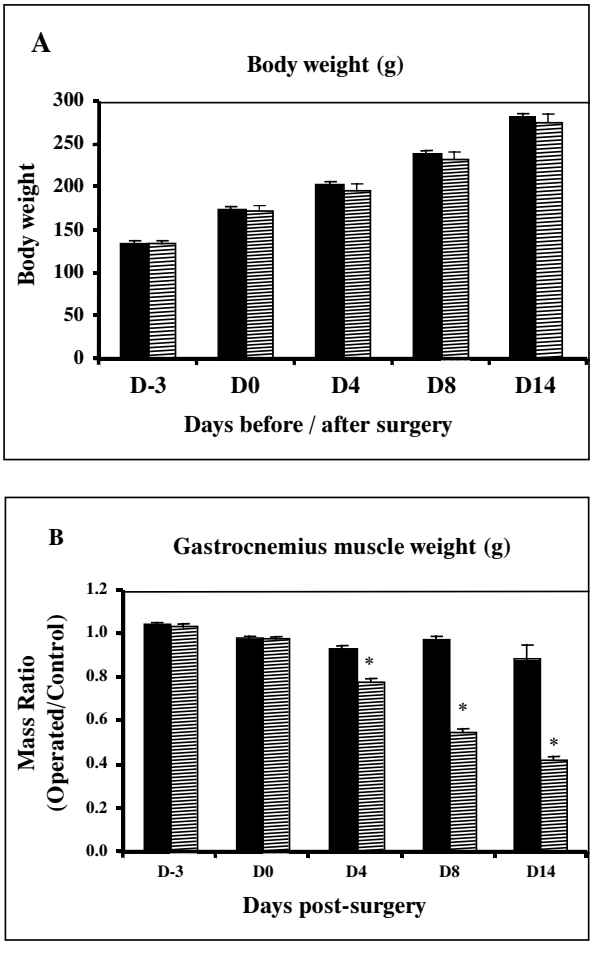

Figure 6. Changes in body weight (A) and gastrocnemius muscle weight (B) following unilateral sciatic neurectomy (USN, hashed bars) or sham-neurectomy (Sham, solid bars). The weight of the gastrocnemius muscle in the operated leg was expressed as a fraction of that in the non-operated leg in the same animal. Data are expressed as mean ± SEM. * $p < 0.05$ between USN and Sham values (n = 6).

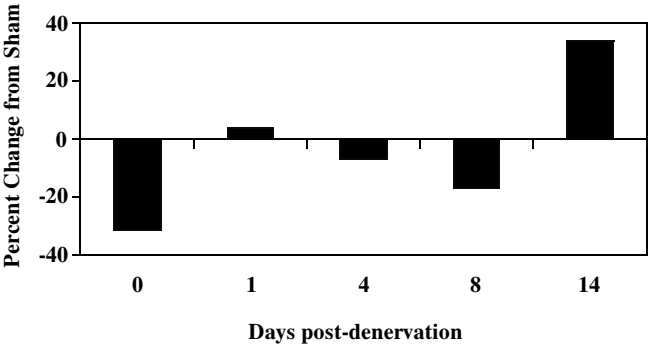

Figure 7. Changes in mRNA levels following denervation-induced muscle atrophy. mRNA was quantified by real-time PCR after cDNA synthesis. Percent change was calculated according to the following formulae: For upregulation, % increase = $(2^{-\Delta\Delta C_t} - 1) \times 100$; For downregulation, % decrease = $((1/2^{-\Delta\Delta C_t} + 1)-1) \times 100$ where $\Delta\Delta C_t$ equals (C_t sample 1 - C_t 18S sample 1) - (C_t sample 2 - C_t 18S sample 2). As a result of this formula, the standard errors could not be calculated. The level of myostatin mRNA in the denervated gastrocnemius muscle was expressed as percent change from that in the sham-denervated muscle (n=6).

the expression of the 42, 30, 15 and 17 kDa species of myostatin in the gastrocnemius, the levels of which paralleled those of the transcript. That is, the levels of myostatin protein in the gastrocnemius muscle were decreased at day 0 and elevated by day 14 following denervation compared with sham-operated controls (Figure 8).

Discussion

The hypothesis that myostatin is a negative regulator of skeletal muscle mass[5,8] derives almost solely from studies in which myostatin activity was manipulated during embryonic development. Only recently has it been shown more directly that myostatin regulates muscle mass postnatally[13] further supporting the potential for myostatin as a target for therapeutic intervention to prevent or treat sarcopenia. For the latter to hold true, however, elevated levels of myostatin protein would be expected in various conditions of sarcopenia, whether due to normal aging, denervation or cachectic states, irrespective of the initiating etiology. To test this hypothesis, this study investigated the levels of expression of myostatin mRNA and protein in age-related sarcopenia as well as in denervation-induced atrophy in young adult rats, in both of which conditions there was approximately 50% muscle atrophy.

In this study, the level of expression of myostatin was examined at both the transcript (mRNA) and protein levels. Myostatin mRNA expression was evaluated by Taqman PCR and confirmed by Northern blot using primers and probes, respectively, that discriminate between myostatin and GDF-11. It should be mentioned that the quantitative PCR technique employed is highly specific and it would be extremely unlikely that the amplicon is anything other than myostatin. The level of myostatin protein expression was estimated by Western blotting using a polyclonal antibody directed against a peptide in the carboxy-terminus. This antibody recognized four immunoreactive species in the gastrocnemius muscle under reducing conditions, sized 15, 17, 30 and 42 kDa. These sizes correspond to expected molecular masses of a monomer (two isoforms), dimer and unprocessed protein, consistent with reports on other members of the TGF-β superfamily[24]. The phenomenon of two low molecular mass species has been reported for osteogenic protein-1 (OP-1, BMP-7) and was attributed to either differential glycosylation or the existence of dynamic intrachain disulfide bonding in the "cysteine knot" that could result from the close proximity of all cysteine residues in the folded protein[24,25]. Additionally, in teleost fishes, two different

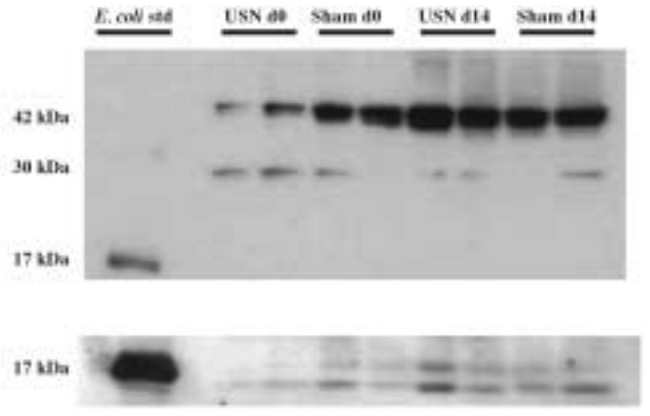

Figure 8. Western blot of gastrocnemius muscles from denervated (USN) and sham-denervated leg of rats at days 0 (6-8 hr) and 14 after the operation. Twenty μg of muscle homogenate was run on a 14% Tris-glycine gel and Western analysis was carried out as described under Materials and Methods. The lower panel shows a longer exposure, which was needed to visualize the lower MW species. The expression of myostatin protein in the denervated gastrocnemius muscle paralleled that of myostatin mRNA.

genes have recently been identified for myostatin[26]. The carboxy-terminal domain of murine myostatin expressed in *E. coli* that was used as control ran predominantly at 17 kDa and a weaker band which represents incompletely reduced dimer was visible at 30 kDa. Previous studies had reported a 28-30 kDa band as well as a 49 kDa band in rat tibialis muscles with no traces of the 14-17 kDa bands[15]. In the rat soleus and extensor digitorum longus muscles, an 18-19 kDa band of myostatin was identified[19]. Also in the rat, a single polypeptide at approximately 35 kDa and 37 kDa were identified, respectively, in the plantaris and soleus muscles[16]. On the other hand, a 26-kDa myostatin-immunoreactive species was identified in the quadriceps muscle of HIV-infected men with wasting[10] as well as in the diaphragm, soleus, tibialis and extensor digitorum longus muscles of the rat[17]. The reasons for the discrepancies in the reported sizes of the myostatin protein are not known.

The present study addressed the issue of specificity of the antibody used for the Western blot analysis and showed that the bands visualized were myostatin and not GDF-11. Thus, the results indicate that in rat skeletal muscle the levels of myostatin protein increases while the level of myostatin mRNA decreases with aging, indicating possible accumulation in the extracellular matrix. These age-related changes in the expression of myostatin transcript and protein occurred with atrophy of the gastrocnemius muscle. In contrast, denervation-induced atrophy of the gastrocnemius muscle in young rats which was apparent by days 4, 8 and 14 after sciatic neurectomy, was not associated with elevation of myostatin mRNA or protein until day 14. Moreover, unlike in aging where the increase in levels of myostatin protein and transcripts varied inversely, in denervation-induced atrophy the changes in myostatin protein and transcripts varied in parallel. These discrepancies between age- and denervation-induced atrophy may be reflective of the rates of onset and progression of muscle atrophy in these conditions. They may also suggest that myostatin might be playing different roles or be differentially regulated in age-induced versus denervation-induced sarcopenia.

The sarcopenia of aging is insidious in onset, usually beginning some time between the fifth and seventh decade of life and progressing until death. It is often accompanied by changes in the expression and function of several genes and proteins including those of growth factors such as insulin and insulin-like growth factor, those involved in excitation-contraction coupling such as the ryanodine and dihydropyridine receptors[27], and myogenic regulatory factors such as myogenin[28,29]. However, although myostatin is hypothesized to negatively regulate skeletal muscle mass and to be a potential mediator of the sarcopenia of aging, there is a dearth of reports on the expression of myostatin transcript or protein in age-related sarcopenia[30,31]. The present finding of increased levels of myostatin protein appears consistent with myostatin being a negative regulator of muscle mass despite the paradoxical decline in the expression of myostatin mRNA with aging. The decline in myostatin mRNA may reflect a negative feedback on transcription arising from the accumulation of latent myostatin protein in the extracellular matrix. Similar accumulations of protein in the extracellular matrix and binding to matrix components have been reported for other members of the TGF-β superfamily of secreted proteins[32-34]. Thus, a similar pattern of expression of the genes and protein of myostatin would be expected in other conditions associated with slowly progressive muscle wasting. Indeed, although the level of expression of myostatin mRNA was not reported, myostatin-immunoreactive proteins were elevated in both the quadriceps muscle and blood of humans with HIV-induced cachexia[10].

In contrast with aging, denervation-induced atrophy is rapid in onset. In the rat gastrocnemius muscle, significant atrophy was present as early as four days after denervation at a time when the level of expression of the transcript or protein of myostatin was suppressed or unchanged relative to sham-operated muscles. These findings are in partial agreement with a previous report that the level of myostatin protein increased slightly at days 4 and 28 after denervation-induced atrophy of the gastrocnemius muscle in the rat[17]. Although the expression of both myostatin mRNA and protein became elevated by day 14 after denervation, the lack of increase in their expression earlier, as well as the small magnitude of the increase, would appear to argue against a major role for myostatin in the etiology of the atrophy. However, it is possible that rapid processing and usage of stored precursor myostatin resulted in its depletion without adequate time for increasing either its mRNA or protein synthesis/accumulation. Detailed studies of the rate of synthesis, storage, processing, usage and degradation of myostatin following denervation will be necessary to address this

possibility. Alternatively, it is possible that myostatin acts as the chalone that regulates muscle mass[8]. In this scenario, myostatin message, protein and activity would increase in response to hypertrophy and decrease in response to atrophy. In partial support of this hypothesis, mechanical overloading that produced over 30-76% hypertrophy of the plantaris muscle was associated with elevated levels of myostatin protein[17]. These conflicting reports confound elucidation of the role of myostatin in regulating muscle mass postnatally and may well reflect the difficulties in separating the effects of myostatin from the complex interplay that it shares with other growth factors such as IGF-I and growth hormone[35].

In summary, the present study showed for the first time that the expression of myostatin protein is elevated in age-related sarcopenia, and that the mRNA and protein are differentially expressed in two models of atrophy that have varying rates of onset. This finding provides support for the prospect of using inhibitors of myostatin to prevent or reverse the slowly progressive sarcopenia that occurs in aging, cancer and HIV-induced cachexia.

Acknowledgments

We thank Mohammed Morsey and Craig Findly for antisera against myostatin, Peter LeMotte, Doug Tan, Boris Chrunyk, and Michele Rosner for purified recombinant E.coli myostatin, and Kim Johnson for helpful input about Taqman.

References

1. Miyazono K, Kusanagi K, Inoue H. Divergence and convergence of TGF-beta/BMP signaling. J Cell Physiol 2001; 187: 265-276.
2. Ji S, Losinski RL, Cornelius SG, Frank GR, Willis GM, Gerrard DE, Depreux FF, Spurlock ME. Myostatin expression in porcine tissues: tissue specificity and developmental and postnatal regulation. Am J Physiol 1998; 275:R1265-1273.
3. Sharma M, Kambadur R, Matthews KG, Somers WG, Devlin GP, Conaglen JV, Fowke PJ, Bass JJ. Myostatin, a transforming growth factor-beta superfamily member, is expressed in heart muscle and is upregulated in cardiomyocytes after infarct. J Cell Physiol 1999; 180:1-9.
4. McPherron AC, Lawler AM, Lee SJ. Regulation of skeletal muscle mass in mice by a new TGF-β superfamily member. Nature 1997; 387:83-90.
5. McPherron AC, Lee SJ. Double muscling in cattle due to mutations in the myostatin gene. Proc Natl Acad Sci U S A 1997; 94:12457-12461.
6. Kambadur R, Sharma M, Smith TP, Bass JJ. Mutations in myostatin (GDF8) in double-muscled Belgian Blue and Piedmontese cattle. Genome Res 1997; 7:910-916.
7. Grobet L, Martin LJ, Poncelet D, Pirottin D, Brouwers B, Riquet J, Schoeberlein A, Dunner S, Menissier F, Massabanda J, Fries R, Hanset R, Georges M. A deletion in the bovine myostatin gene causes the double-muscled phenotype in cattle. Nat Genet 1997; 17:71-74.
8. Lee SJ, McPherron AC. Myostatin and the control of skeletal muscle mass. Curr Opin Genet Dev 1999; 9:604-607.
9. Zhu X, Hadhazy M, Wehling M, Tidball JG, McNally EM. Dominant negative myostatin produces hypertrophy without hyperplasia in muscle. FEBS Lett 2000; 474:71-75.
10. Gonzalez-Cadavid NF, Taylor WE, Yarasheski K, Sinha-Hikim I, Ma K, Ezzat S, Shen R, Lalani R, Asa S, Mamita M, Nair G, Arver S, Bhasin S. Organization of the human myostatin gene and expression in healthy men and HIV-infected men with muscle wasting. Proc Natl Acad Sci U S A 1998; 95:14938-14943.
11. Zachwieja JJ, Smith SR, Sinha-Hikim I, Gonzalez-Cadavid N, Bhasin S. Plasma myostatin-immunoreactive protein is increased after prolonged bed rest with low-dose T3 administration. J Gravit Physiol 1999; 6:11-15.
12. Reardon KA, Davis J, Kapsa RM, Choong P, Byrne E. Myostatin, insulin-like growth factor-1, and leukemia inhibitory factor mRNAs are upregulated in chronic human disuse muscle atrophy. Muscle Nerve 2001; 24:893-899.
13. Zimmers TA, Davies MV, Koniaris LG, Haynes P, Esquela AF, Tomkinson KN, McPherron AC, Wolfman NM, Lee SJ. Induction of cachexia in mice by systemically administered myostatin. Science 2002; 296:1486-1488.
14. Carlson CJ, Booth FW, Gordon SE. Skeletal muscle myostatin mRNA expression is fiber-type specific and increases during hindlimb unloading. Am J Physiol 1999; 277:R601-R606.
15. Lalani R, Bhasin S, Byhower F, Tarnuzzer R, Grant M, Shen R, Asa S, Ezzat S, Gonzalez-Cadavid NF. Myostatin and insulin-like growth factor-I and -II expression in the muscle of rats exposed to the microgravity environment of the NeuroLab space shuttle flight. J Endocrinol 2000; 167:417-428.
16. Wehling M, Cai B, Tidball JG. Modulation of myostatin expression during modified muscle use. FASEB J 2000; 14:103-110.
17. Sakuma K, Watanabe K, Sano M, Uramoto I, Totsuka T. Differential adaptation of growth and differentiation factor 8/myostatin, fibroblast growth factor 6 and leukemia inhibitory factor in overloaded, regenerating and denervated rat muscles. Biochim Biophys Acta 2000; 1497:77-88.
18. Yamanouchi K, Soeta C, Naito K, Tojo H. Expression of myostatin gene in regenerating skeletal muscle of the rat and its localization. Biochem Biophys Res Commun 2000; 270:510-516.
19. Mendler L, Zador E, Ver Heyen M, Dux L, Wuytack F. Myostatin levels in regenerating rat muscles and in myogenic cell cultures. J Muscle Res Cell Motil 2000; 21:551-563.
20. Peppel K, Baglioni C. A simple and fast method to extract RNA from tissue culture cells. Biotechniques 1990; 9:711-713.
21. Applied Biosystems. User Bulletin #2: ABI Prism Sequence Detection System. Technical Bulletin; 1997.
22. Sambrook J, Fritsch E, Maniatis T. Molecular Cloning: A Laboratory Manual. Cold Spring Harbor Laboratory Press; 1989.
23. Paralkar VM, Vail AL, Grasser WA, Brown TA, Xu H, Vukicevic S, Ke HZ, Owen T, Thompson DD. Cloning and characterization of a novel member of the transforming growth factor beta/bone morphogenetic protein family. J Biol Chem 1998; 273:13760-13767.
24. Sampath TK, Maliakal JC, Hauschka PV, Jones WK, Sasak H, Tucker RF, White KH, Coughlin JE, Tucker MM, Pang RH. Recombinant human osteogenic protein-1 (hOP-1) induces new bone formation *in vivo* with a specific activity comparable with natural bovine osteogenic protein and stimulates osteoblast proliferation and differentiation *in vitro*. J Biol Chem 1992; 267:20352-20362.

25. Jones WK, Richmond EA, White K, Sasak H, Kusmik W, Smart J, Oppermann H, Rueger DC, Tucker RF. Osteogenic protein-1 (OP-1) expression and processing in Chinese hamster ovary cells: isolation of a soluble complex containing the mature and pro-domains of OP-1. Growth Factors 1994; 11:215-225.
26. Maccatrozzo L, Bargelloni L, Cardazzo B, Rizzo G, Patarnello T. A novel second myostatin gene is present in teleost fish. FEBS Lett 2001; 509:36-40.
27. Delbono O. Regulation of excitation contraction coupling by insulin-like growth factor-1 in aging skeletal muscle. J Nutr Health Aging 2000; 4:162-164.
28. Marsh DR, Criswell DS, Carson JA, Booth FW. Myogenic regulatory factors during regeneration of skeletal muscle in young, adult, and old rats. J Appl Physiol 1997; 83:1270-1275.
29. Kostrominova TY, Macpherson PC, Carlson BM, Goldman D. Regulation of myogenin protein expression in denervated muscles from young and old rats. Am J Physiol Regul Integr Comp Physiol 2000; 279:R179-188.
30. Mallidis C, Bhasin S, Matsumoto A, Shen R, Gonzalez-Cadavid NF. Skeletal muscle myostatin in a rat model of aging-associated sarcopenia. The Endocrine Society 81st Annual Meeting Proceedings 1999; Abstract OR9-1.
31. Yarasheski K, Bhasin S, Sinha-Hikim I, Pak-Loduca J, Gonzalez-Cadavid N. Serum myostatin-immunoreactive protein is increased with muscle wasting and advanced age. The Endocrine Society 81st Annual Meeting Proceedings 1999; Abstract OR9-2.
32. Paralkar VM, Nandedkar AK, Pointer RH, Kleinman HK, Reddi AH. Interaction of osteogenin, a heparin binding bone morphogenetic protein, with type IV collagen. J Biol Chem 1990; 265:17281-17284.
33. Paralkar VM, Slobodan V, Reddi HA. Transforming growth factor beta type I binds to collagen IV of basement membrane matrix: implications for development. Dev Biol 1991; 143:303-308.
34. Yamaguchi Y, Mann DM, Ruoslahti E. Negative regulation of transforming growth factor-beta by the proteoglycan decorin. Nature 1990; 346:281-284.
35. Marcell TJ, Harman SM, Urban RJ, Metz DD, Rodgers BD, Blackman MR. Comparison of GH, IGF-I, and testosterone with mRNA of receptors and myostatin in skeletal muscle in older men. Am J Physiol Endocrinol Metab 2001; 281:E1159-1164.